Nonlinear Dyn (2015) 80:1091–1108
DOI 10.1007/s11071-015-1929-0

ORIGINAL PAPER

Effect of multi-phase optimal velocity function on jamming transition in a lattice hydrodynamic model with passing

Arvind Kumar Gupta · Sapna Sharma · Poonam Redhu

Received: 29 May 2014 / Accepted: 14 January 2015 / Published online: 29 January 2015

Abstract In this paper, we study the effect of multi-phase optimal velocity function on a density difference lattice model with passing. The effect of reaction coefficient is examined through linear stability analysis and shown that it can significantly enlarge the stability region on the phase diagram for any rate of passing. Using nonlinear stability analysis, the critical value of passing constant is obtained and found independent of reaction coefficient. Below this critical value for which kink soliton solution of mKdV equation exists. By varying the density, multiple phase transitions are analyzed, which highly depend on the sensitivity, reaction coefficient and passing constant. It is observed that the number of stages in multi-phase transitions closely related to the number of the turning points in the optimal velocity function. The theoretical findings are verified using numerical simulation, which confirm that phase diagrams of multi-phase traffic in the case of passing highly depend on the choice of optimal velocity function as well as on other parameters such as sensitivity, reaction coefficient and rate of passing.

Keywords Traffic flow · Optimal velocity function · Chaotic jam

A. K. Gupta (✉) · P. Redhu
Indian Institute of Technology Ropar, Rupnagar 140001, Punjab, India
e-mail: akgupta@iitrpr.ac.in

P. Redhu
e-mail: poonamr@iitrpr.ac.in

S. Sharma
Department of Mathematics, DAV University, Jalandhar 144012, India
e-mail: sapna2002@gmail.com

S. Sharma
School of Mathematical Sciences, University of Science and Technology of China, Hefei 230026, China

1 Introduction

In recent years, due to rapid increase of automobiles on the roads, the problem of traffic congestion has attracted considerable attention of scientists and researchers. Therefore, a considerable variety of traffic models [1–14] have been discussed to study the complex phenomena as a typical example of nonequilibrium statistical physics of self-driven many-particle systems. Nagatani [15] firstly introduced a lattice hydrodynamic model in which drivers adjust their velocity according to the observed headway. Later, many extended version of Nagatani's lattice model have been developed by considering different factors such as density difference effect [16], backward effect [17], lateral effect of the lane width [18], effect of passing rate [19] and anticipation effect of potential lane changing [20]. Most of the above-cited models describe some traffic phenomena only on single-lane or two-lane highway. Furthermore, Nagatani also extended his original lattice model to two-lane traffic system and analyzed the lane-changing behavior [21]. After that, some improvements

have been made to validate the model under real traffic situations, and accordingly, many relatively more reasonable models have been developed. In this direction, some modifications have also been proposed by considering optimal current difference [22], density difference effect [23] and effect of driver's anticipation [24] in two-lane system. Recently, Gupta and Redhu [25] developed a new model by considering driver's anticipation effect in sensing relative flux (DAESRF) in a two-lane system.

Generally in all the above models, traffic characteristics have been studied using linear as well as nonlinear analysis and the density wave in the congestion region is defined in terms of mKdV equation. It is shown that the jamming transition is similar to the conventional phase transition having two traffic phases and one coexisting phase: free flow, homogeneous congested flow and inhomogeneous flow. However, the fundamental models fail to validate the empirical evidence [26].

In lattice hydrodynamic models, the neutral stability curve highly depends on the optimal velocity function that often chosen as a simple hyperbolic tangent function of the density, depicting the simple acceleration of a vehicle. As a result, all the existing models exhibit the conventional jamming transitions between two traffic phases corresponding to gas, liquid and gas–liquid transition. In the car-following model, Nagatani [27] also pointed out that a driver accelerates or decelerates his/her vehicle by the use of the accelerator, gear lever or brake. As a result, a vehicle's behavior is more complex than the simple optimal velocity function. In this direction, Nagai et al. [28] investigated the effect of stepwise accelerations on the jamming transition in the extended car-following model. Li et al. [29] analyzed the effect of modified multi-phase optimal velocity function on phase transition in a lattice hydrodynamic model. But, upto our knowledge, the effect of multi-phase optimal velocity model has not been studied in traffic systems with passing. In this paper, from the viewpoint of lattice hydrodynamic traffic flow, we firstly extend a more accurate DDLM lattice model to consider the passing effect and then investigate the influence of a multi-phase optimal velocity function on traffic phase transition.

The paper is organized as follows: In the following section, a more realistic lattice model considering the density difference effect between the leading and the following lattice with passing for a single lane is proposed. In Sect. 3, the linear stability analysis is performed for the proposed model. Section 4 is devoted to the nonlinear analysis in which mKdV equation is derived. Numerical simulations are carried out in Sect. 5, and finally, conclusions are given in Sect. 6.

2 Proposed model

Nagatani [15] introduced the first lattice hydrodynamic model by incorporating both the ideas of car-following models and macroscopic models to analyze the density wave of traffic flow and is given by

$$\partial_t \rho_j + \rho_0(\rho_j v_j - \rho_{j-1} v_{j-1}) = 0, \tag{1}$$

$$\partial_t(\rho_j v_j) = a[\rho_0 V(\rho_{j+1}) - \rho_j v_j], \tag{2}$$

where j indicates site-j on the one-dimensional lattice; ρ_j and v_j, respectively, represent the local density and velocity at site-j at time t; ρ_0 is the average density; $a(=1/\tau)$ is the sensitivity of drivers; and $V(.)$ is called optimal velocity function.

Later, the above model is further modified by Tian et al. [16] by introducing density difference term in the evolution equation as follows:

$$\partial_t \rho_j + \rho_0(\rho_j v_j - \rho_{j-1} v_{j-1}) = 0, \tag{3}$$

$$\partial_t(\rho_j v_j) = a[\rho_0 V(\rho_{j+1}) - \rho_j v_j] + \lambda(\rho_j - \rho_{j-1})/\rho_0, \tag{4}$$

where λ is the reaction coefficient to the density difference. The stable region of the above density difference lattice model (DDLM) in the phase diagram was found larger than that of Nagatani's model, and vehicle dynamics also become more realistic than Nagatani's model. On the other hand, to make the model more realistic, Nagatani extended his model to consider the passing effect in one-dimensional traffic flow. The continuity equation remains preserved even in the passing case while the evolution equation is modified by looking at the difference of traffic currents on site-j and $j+1$. When the traffic current on site-j is larger than the current on site-$j+1$, passing occurs and is proportional to the difference between the optimal currents at site-j and $j+1$. However, the above-discussed density difference effect was not considered in the Nagatani's model with passing. In view this, we proposed a new evolution equation with consideration of density difference effect on one-dimensional traffic flow when passing is allowed as follows:

$$\begin{aligned}\partial_t(\rho_j v_j) =& a[\rho_0 V(\rho_{j+1}(t)) - \rho_j v_j(t)] \\ &+ \lambda(\rho_j - \rho_{j-1})/\rho_0 \\ &+ a\gamma\left[\rho_0 V(\rho_{j+1}(t)) - \rho_0 V(\rho_{j+2}(t))\right],\end{aligned} \tag{5}$$

where γ is a passing constant. By taking the difference form of Eqs. (3) and (5) and eliminating speed v_j, the evolution equation of density is obtained as

$$\begin{aligned}&\partial_t^2\rho_j(t) + a\partial_t\rho_j(t) + a\rho_0^2\left[V(\rho_{j+1}(t)) - V(\rho_j(t))\right] \\ &-\lambda\Delta^2\rho_{j-1}(t) + a\gamma\rho_0^2[2V(\rho_{j+1}(t)) - V(\rho_{j+2}(t)) \\ &-V(\rho_j(t))] = 0,\end{aligned} \tag{6}$$

where $\Delta\rho_j(t) = \rho_{j+1}(t) - \rho_j(t)$, $V'(\rho_j) = \mathrm{d}V/\mathrm{d}\rho_j$.

It is clear from the above Eq. (6) that the density at any site not only depends on forward and backward lattice but also significantly affected by the choice of optimal velocity function. In almost all lattice hydrodynamic models, the following conventional two-phase optimal velocity function depicting the simple acceleration of a vehicle is adopted as

$$V(\rho) = \frac{V_{\max}}{2}\left[\tanh\left(\frac{1}{\rho} - \frac{1}{\rho_c}\right) + \tanh\left(\frac{1}{\rho_c}\right)\right], \tag{7}$$

where, $V_{\max}$ and ρ_c denote the maximal velocity and the safety critical density, respectively. This optimal velocity function is monotonically decreasing and has an upper bound and an inflection point at $\rho = \rho_c = \rho_0$. The above optimal velocity function is able to explain the simple jamming transitions among the free traffic, inhomogeneous traffic and congested traffic. However, real traffic flow shows very complex traffic behavior than that of two-phase traffic. Moreover, a driver accelerates or decelerates his/her vehicle by the use of the accelerator, gear lever or brake, which leads to a more complex vehicle's behavior than the simple optimal velocity function. In this direction, Nagai et al. [28] also investigated the effect of stepwise accelerations by choosing multi-phase optimal velocity function on the jamming transition in a car-following model. The following two-stage (three-phase) optimal velocity model is proposed:

$$V(\rho) = \frac{V_{\max}}{4}\sum_{i=1}^{i=2}\left[\tanh\left(\frac{\alpha_i}{\rho} - \frac{\alpha_i}{\rho_{c_i}}\right) + \tanh\left(\frac{\alpha_i}{\rho_{c_i}}\right)\right]. \tag{8}$$

For simplicity, the following parameters are chosen: $\alpha_1 = \alpha_2 = 2.0$, $\rho_{c_1} = 0.15$, and $\rho_{c_2} = 0.25$. Note that the modified optimal velocity function (8) has two turning points (inflection points). This is in accordance with the fact that a driver accelerates or decelerates his/her vehicle by the use of the accelerator, gear lever or brake, so the discontinuous accelerations, to some extent, lead to the occurrence of more than one turning point in the optimal velocity function.

3 Linear stability analysis

To investigate the effect of density difference on traffic flow when passing is allowed, we conducted linear stability analysis in this section. The traffic density and optimal velocity under uniform traffic condition are taken as ρ_0 and $V(\rho_0)$, respectively, where ρ_0 is a constant. Hence, the steady-state solution of the homogeneous traffic flow is given by

$$\rho_j(t) = \rho_0, \quad V(\rho_j(t)) = V(\rho_0). \tag{9}$$

Let $y_j(t)$ be a small perturbation to the steady-state density on site-j. Then,

$$\rho_j(t) = \rho_0 + y_j(t). \tag{10}$$

Substituting $\rho_j(t) = \rho_0 + y_j(t)$ in Eq. (6), we obtain

$$\begin{aligned}&\partial_t^2 y_j(t) + a\partial_t y_j(t) + a\rho_0^2 V'(\rho_0)\Delta y_j(t) \\ &- \lambda\Delta^2 y_{j-1}(t) - a\gamma\rho_0^2 V'(\rho_0)\Delta^2 y_j(t) = 0,\end{aligned} \tag{11}$$

where $\Delta y_j(t) = y_{j+1}(t) - y_j(t)$.

Putting $y_j(t) = exp(ikj + zt)$ in Eq. (11), we get

$$\begin{aligned}&z^2 + az + a\rho_0^2 V'(\rho_0)(e^{ik} - 1) + \lambda(2 - e^{ik} - e^{-ik}) \\ &+ a\gamma\rho_0^2 V'(\rho_0)(2e^{ik} - e^{2ik} - 1) = 0,\end{aligned} \tag{12}$$

where k denotes the phase of the perturbation and i is an imaginary number. Inserting $z = z_1(ik) + z_2(ik)^2 \ldots$ into Eq. (12), we obtained the first- and second-order terms of the coefficient ik and $(ik)^2$, respectively, as

$$z_1 = -\rho_0^2 V'(\rho_0), \tag{13}$$

$$z_2 = -\frac{z_1^2}{a} - \frac{\rho_0^2 V'(\rho_0)}{2} + \frac{\lambda}{a} + \gamma\rho_0^2 V'(\rho_0). \tag{14}$$

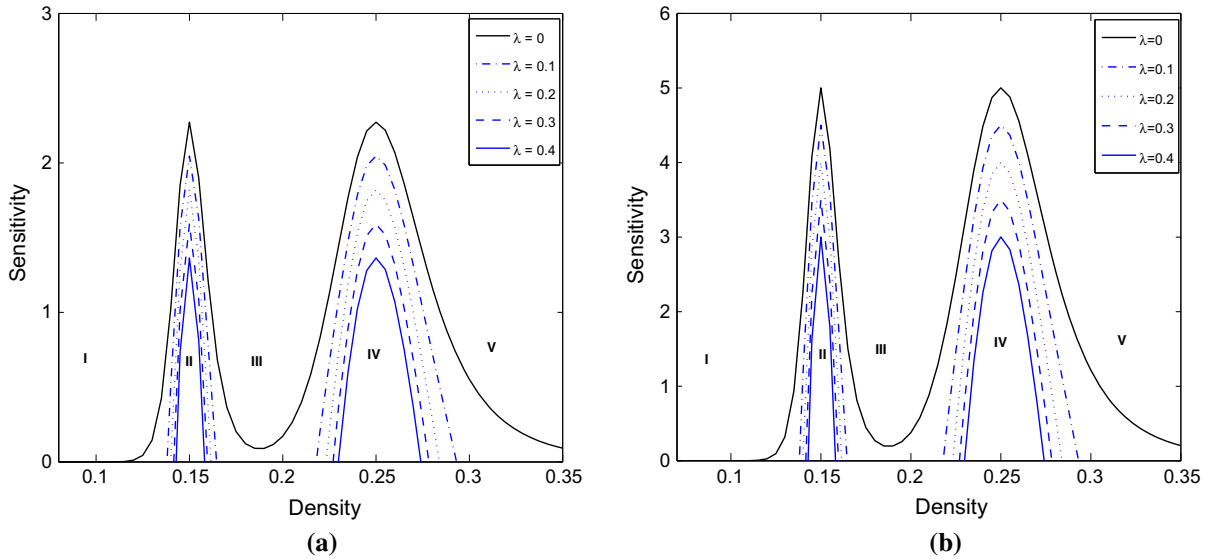

Fig. 1 Phase diagram in parameter space (ρ, a) for **a** $\gamma = 0.06$, and **b** $\gamma = 0.3$, respectively

When $z_2 < 0$, the uniform steady-state flow becomes unstable for long-wavelength waves. For $z_2 > 0$, the uniform flow will remain stable. Thus, the neutral stability curve is given by

$$a = -\frac{2\rho_0^2 V'(\rho_0)}{1-2\gamma} + \frac{2\lambda}{\rho_0^2 V'(\rho_0)(1-2\gamma)}. \tag{15}$$

The instability condition for the homogeneous traffic flow can be described as

$$a < \frac{2(\lambda - \rho_0^4 V'^2(\rho_0))}{(1-2\gamma)\rho_0^2 V'(\rho_0)}. \tag{16}$$

When $\gamma = 0$, the results of instability condition is same as in Ref. [16]. Equation (16) clearly shows that reaction coefficient λ plays an important role in stabilizing the traffic flow when passing is considered. Curves in Fig. 1a, b are the neutral stability curves with two turning points in the phase space (ρ, a) corresponding to $\gamma = 0.06$ and $\gamma = 0.3$, respectively, for different values of λ. The apex of each curve indicates the critical points $[\rho_{c_1}, a_c(\lambda)]$ and $[(\rho_{c_2}, a_c(\lambda)]$. It can be easily depicted from the figure that the amplitude of these curves decreases with an increase in λ, which means that larger value of λ leads to enlargement of stable region, and hence, the traffic jam is suppressed efficiently. On comparing Fig. 1a, b, it is found that the stable region reduces for larger value of the passing coefficient.

4 Nonlinear stability analysis

In this section, we investigate the evolution characteristics by using the method of long-wavelength expansion to describing the collective motion on coarse-grained scales. Assuming, $X = \epsilon(j + bt)$ and $T = \epsilon^3 t$ as the slow variables for scaling parameter ϵ $(0 < \epsilon << 1)$ near the critical point, where b is a constant to be determined. Let the density at site-j near the critical point be

$$\rho_j(t) = \rho_c + \epsilon R(X, T). \tag{17}$$

By expanding Eq. (6) to fifth order of ϵ with the help of Eq. (17), we obtain the following nonlinear equation:

$$\begin{aligned}
&\epsilon^2\left[b + \rho_c^2 V'\right]\partial_X R + \epsilon^3\left[\frac{b^2}{a} + \frac{\rho_c^2 V'}{2}(1-2\gamma) - \frac{\lambda}{a}\right]\partial_X^2 R \\
&+ \epsilon^4\left[\partial_T R + \frac{\rho_c^2 V'}{6}(1-6\gamma)\partial_X^3 R + \frac{\rho_c^2 V'''}{6}\partial_X R^3\right] \\
&+ \epsilon^5\left[\frac{2b^2}{a}\partial_T\partial_X R + \left(\frac{\rho_c^2 V'}{24} - \frac{\lambda}{12a} - \frac{7}{12}\rho_c^2 V'\gamma\right)\partial_X^4 R \right.\\
&\left. + \frac{\rho_c^2 V'''}{12}(1-2\gamma)\partial_X^2 R^3\right] = 0,
\end{aligned} \tag{18}$$

Table 1 The coefficients g_i of the model

g_1	g_2	g_3
$(\frac{1-6\gamma}{6})(-\rho_c^2 V')$	$\frac{\rho_c^2 V'''}{6}$	$\frac{\rho_c^2 V'(1-2\gamma)}{2}$
g_4		g_5
$\frac{b^2(1-6\gamma)(-\rho_c^2 V')}{3a_c}$ $+\frac{(1-14\gamma)\rho_c^2 V'}{24} - \frac{\lambda}{12a_c}$		$\frac{\rho_c^2 V'''}{12}\left(1-2\gamma-\frac{4b^2}{a_c}\right)$

where $V' = \frac{dV(\rho)}{d\rho}|_{\rho=\rho_c}$ and $V''' = \frac{d^3V(\rho)}{d\rho^3}|_{\rho=\rho_c}$. In the neighborhood of critical point a_c, we define

$$a_c = a(1+\epsilon^2), \tag{19}$$

and choosing $b = -\rho_c^2 V'$. Eliminating second- and third-order terms of ϵ into Eq. (18), we get

$$\epsilon^4(\partial_T R - g_1\partial_X^3 R + g_2\partial_X R^3) + \epsilon^5(g_3\partial_X^2 R + g_4\partial_X^4 R + g_5\partial_X^2 R^3) = 0, \tag{20}$$

where the coefficients g_i $(i = 1, 2, \ldots, 5)$ are shown in Table 1. In order to derive the standard mKdV equation, we make the following transformations in Eq. (20):

$$T' = g_1 T, \quad R = \sqrt{\frac{g_1}{g_2}}R', \tag{21}$$

with the existence condition as $g_1 > 0$. After applying the above transformation, Eq. (20) becomes

$$\partial_T R' - \partial_X^3 R' + \partial_X R'^3 + \epsilon M[R'] = 0, \tag{22}$$

where $M[R'] = \frac{1}{g_1}\left(g_3\partial_X^2 R' + \frac{g_1 g_5}{g_2}\partial_X^2 R'^3 + g_4\partial_X^4 R'\right)$. After ignoring the $O(\epsilon)$ terms in Eq. (22), we get standard mKdV equation whose desired kink soliton solution is given by

$$R_0'(X, T') = \sqrt{c}\tanh\sqrt{\frac{c}{2}}(X - cT'). \tag{23}$$

In order to determine the value of propagation velocity for the kink–antikink solution, it is necessary to satisfy the solvability condition:

$$(R_0', M[R_0']) \equiv \int_{-\infty}^{\infty} dX R_0' M[R_0'] = 0, \tag{24}$$

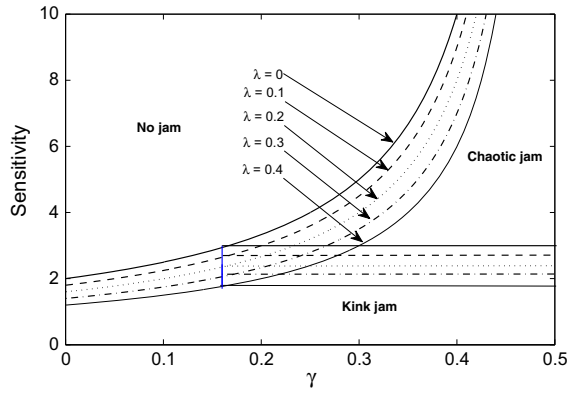

Fig. 2 Phase diagram in parameter space (γ, a)

with $M[R_0'] = M[R']$. By solving Eq. (24), the selected value of c is

$$c = \frac{5g_2 g_3}{2g_2 g_4 - 3g_1 g_5}. \tag{25}$$

Hence, the kink–antikink solution is given by

$$\rho_{j,m}(t) = \rho_c + \epsilon\sqrt{\frac{g_1 c}{g_2}}\tanh\left(\sqrt{\frac{c}{2}}(X - cg_1 T)\right), \tag{26}$$

with $\epsilon^2 = \frac{a_c}{a} - 1$ and the amplitude A of the solution is

$$A = \sqrt{\frac{g_1}{g_2}\epsilon^2 c}. \tag{27}$$

The above kink solution exists only for

$$0 \le \gamma < 0.1667, \tag{28}$$

For $\gamma \ge 0.1667$, the mKdV equation (22) cannot be derived from the above nonlinear analysis. Fig. 2 shows the phase diagram in parameter space (γ, a) for different values of λ. Curves $a_c = 2(1-\lambda)/(1-2\gamma)$, predicated by the linear stability analysis, represent the phase boundaries between no jam and kink jam for $\gamma < 0.1667$ and no jam with chaotic jam for $\gamma \ge 0.1667$. The modified Korteweg de Varies equation (22) has a kink–antikink soliton solution only for $\gamma < 0.1667$; therefore, there exist only two regions no jam and kink jam for $\gamma < 0.1667$ in the phase plane. It is also clear from Fig. 2 that kink region reduces with

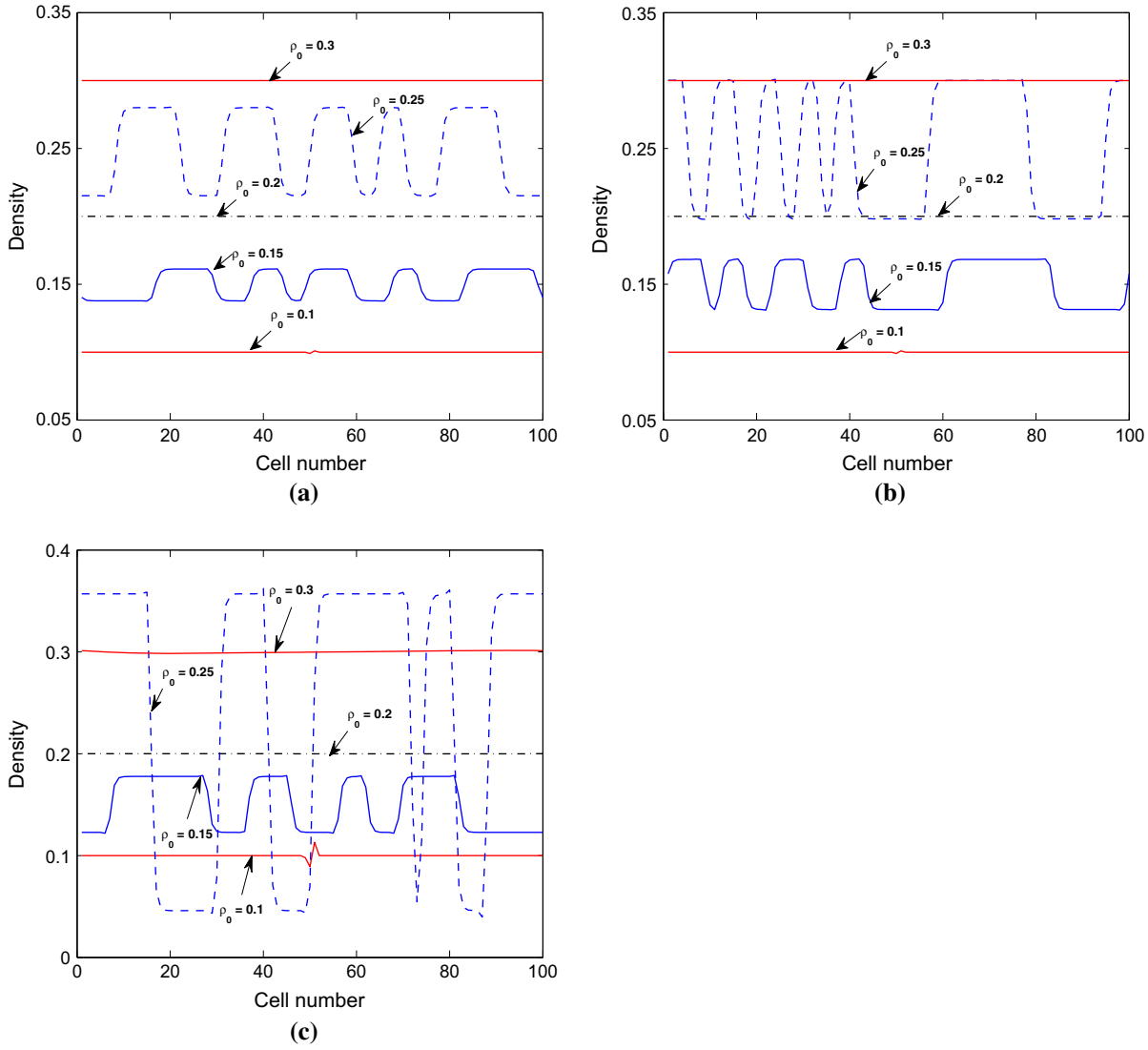

Fig. 3 Density profiles at time $t = 20{,}200$ s when $\gamma = 0.06$ for $\lambda = 0$; **a** $a = 1.72$, **b** $a = 1.2$ and **c** $a = 0.8$, respectively

an increase in the value of λ for $\gamma < 0.1667$. These findings are in accordance with the results obtained in Ref. [25] that traffic jam suppressed efficiently by considering driver's anticipation effect. For $\gamma \geq 0.1667$, based upon the kinds of density wave, the unstable region is further divided into two subregions: kink jam and chaotic jam. The boundary between kink and chaotic jam is the line $a = 2(1-\lambda)/(1-2\gamma)$. It is worth to mention here that for $\lambda = 0$, the results are similar to those obtained in Ref. [19]. The reaction coefficient λ also plays an important role when passing rate is high ($\gamma \geq 0.1667$). The increase in the value of λ enlarges the free flow region while the chaotic and kink jam region reduces.

5 Numerical simulation

To check the effect of multi-phase optimal velocity function on the jamming transition of traffic flow when passing is allowed and validate linear as well as nonlinear stability analysis, numerical simulation is carried out for the proposed model under periodic boundary conditions. We use nonrandom initial conditions and defined density in terms of a step function as:

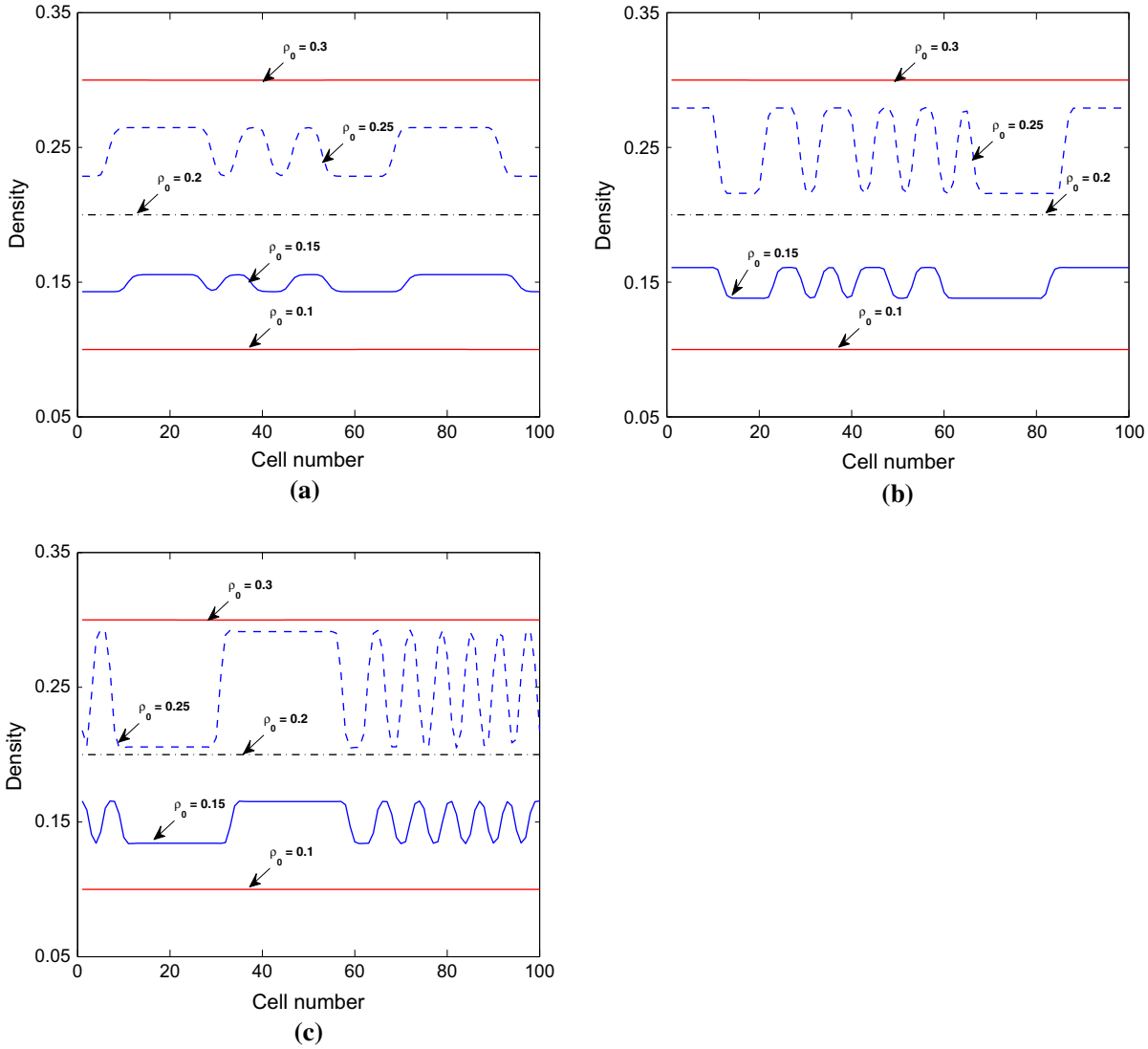

Fig. 4 Density profiles at time $t = 20{,}200$ s when $\gamma = 0.06$ for $\lambda = 0.2$; **a** $a = 1.72$, **b** $a = 1.2$ and **c** $a = 0.8$, respectively

$$\rho_j(1) = \rho_j(0) = \begin{cases} \rho_0; & j \neq \frac{L}{2}, \frac{L}{2}+1 \\ \rho_0 - \sigma; & j = \frac{L}{2} \\ \rho_0 + \sigma; & j = \frac{L}{2}+1 \end{cases}$$

where σ is the initial disturbance and constant and L is the total number of sites taken as 100. The value of the parameters are chosen as : $\sigma = 0.05$ and $V_{\max} = 2.0$. From nonlinear stability analysis, it is derived that kink soliton solution of mKdV equation exists only for $0 \leq \gamma < 0.1667$. Therefore, we presented the discussion on results for two different range of γ.

Case 1: $0 \leq \gamma < 0.1667$

First, we investigate the density profile by varying initial density after sufficiently long time, namely 2×10^4 s steps for different sets of λ and sensitivity on traffic system when passing is allowed at a smaller rate.

If the sensitivity is more than $a_c(\lambda)$, the traffic flow is stable and density evolves in time to a uniform profile regardless of any disturbance in the initial profile. There does not occur any type of phase transition in such case for any choice of initial density. When $a < a_c(\lambda)$, the complex behavior of traffic flow is observed. Figures 3 and 4 show the density profiles

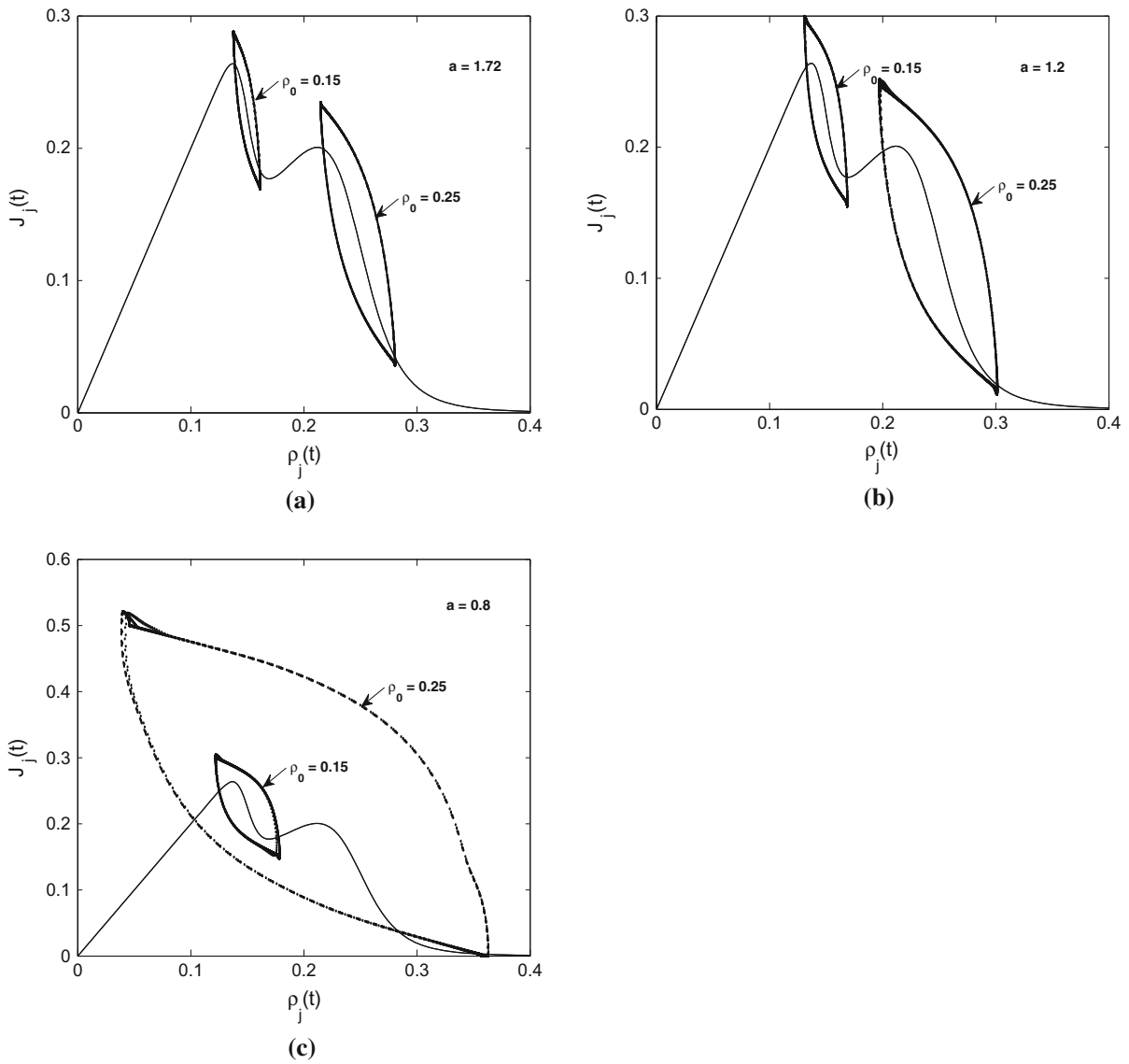

Fig. 5 Plot of $q_j(t)$ against $\rho_j(t)$ when $\gamma = 0.06$ for $\lambda = 0$; **a** $a = 1.72$, **b** $a = 1.2$ and **c** $a = 0.8$, respectively

for different sensitivities corresponding to two different values of $\lambda = 0$ and 0.2, respectively, by varying the initial densities as $\rho_j(0) = 0.1, 0.15, 0.2, 0.25$, and 0.3. At $\rho_j(0) = 0.1$, the stability criterion is satisfied and the traffic is in stable state (Phase I) exhibiting the homogeneous free flow. With an increase in the initial density to $\rho_j(0) = 0.15$, the traffic becomes unstable representing the coexisting phase of Phases I and II. The initial disturbances lead to the kink–antikink soliton which propagates in the backward direction. For an intermediate initial density $\rho_j(0) = 0.2$, the traffic again becomes homogeneous exhibiting the stable state (Phase II). Further increase in density leads to the second homogeneous coexisting phase of Phases II and III. At $\rho_j(0) = 0.3$, the traffic again becomes stable and results in the homogeneous congested state (Phase III). Here, the phase transitions occur in four stages: For low density, the dynamic phase transitions occur from free flow (Phase I) to intermediate homogeneous congested traffic (Phase II) through inhomogeneous traffic (coexistence of Phase I and II). While for the high density, the phase transitions occur from intermediate homo-

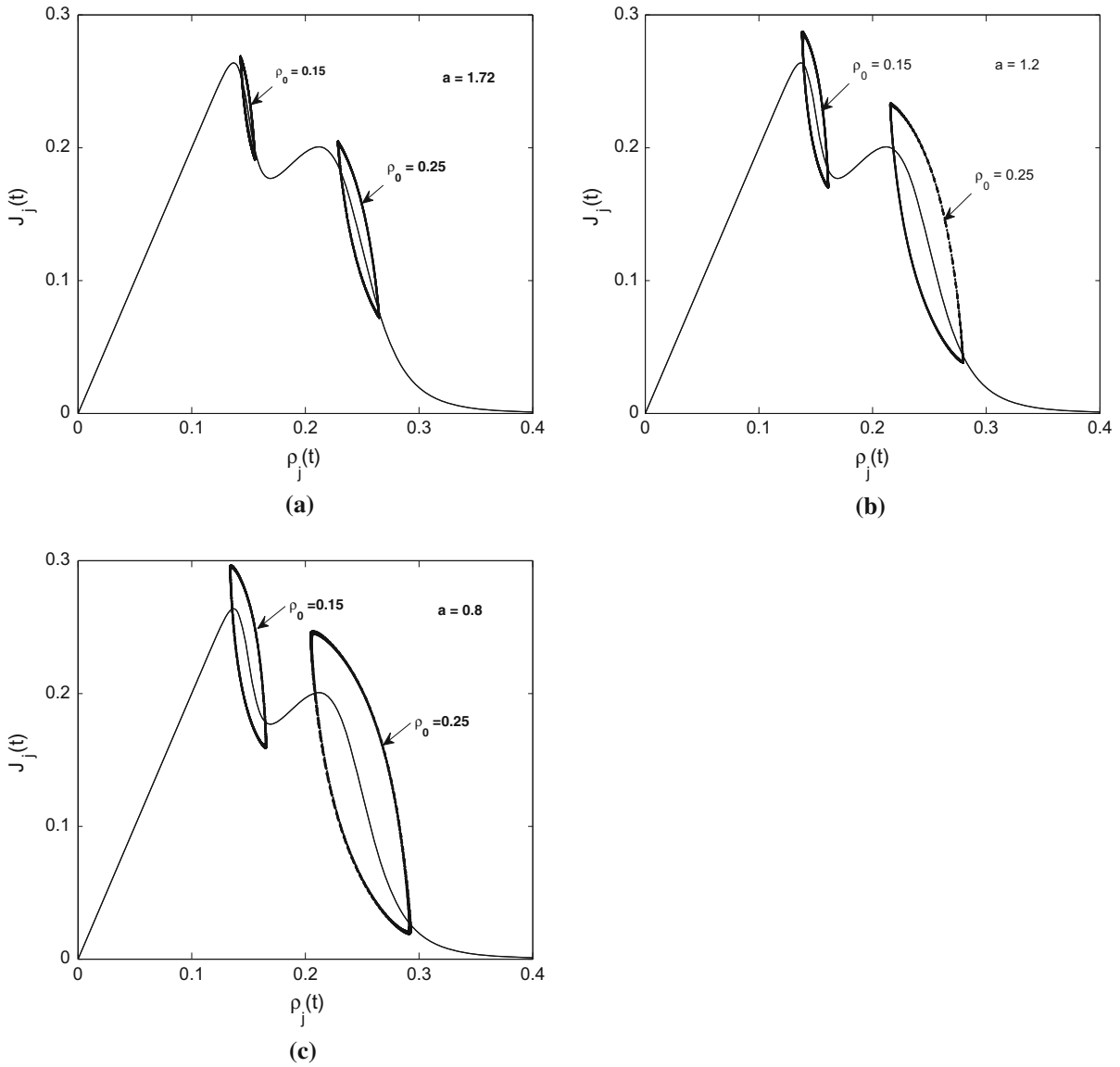

Fig. 6 Plot of $q_j(t)$ against $\rho_j(t)$ when $\gamma = 0.06$ for $\lambda = 0.2$; **a** $a = 1.72$, **b** $a = 1.2$ and **c** $a = 0.8$, respectively

geneous congested traffic (Phase II) to homogeneous congested traffic (Phase III) through inhomogeneous traffic (coexistence of Phase II and III). It is worth to mention that there exist tri-stable states which represent the novel characteristic of many-particle system. Here, the traffic dynamics display the characteristics of three-phase traffic along with two coexisting phases.

It is also clear from the Figs. 3 and 4 that increase in λ leads to decrease in the amplitude of the density waves in both the coexisting regions. This verifies the fact that λ has a stabilizing effect on traffic flow. The effect of sensitivity on traffic flow for two different values of λ can also be observed from the Figs. 3a–c and 4a–c. The amplitude of the density waves increases with a decrease in the sensitivity for any value of λ. It is to be noted that in second coexisting region density waves amplified largely as compared to those occurred in first coexisting region. In addition, one can observe from the figure that the amplitude of the density wave in second coexisting region is always larger than that of in the first coexisting region for all values of λ and sensitivity. It is due to the fact that initial small amplitude disturbance can evolve into congested flow more easily in the high density region where the traffic flow is more unstable.

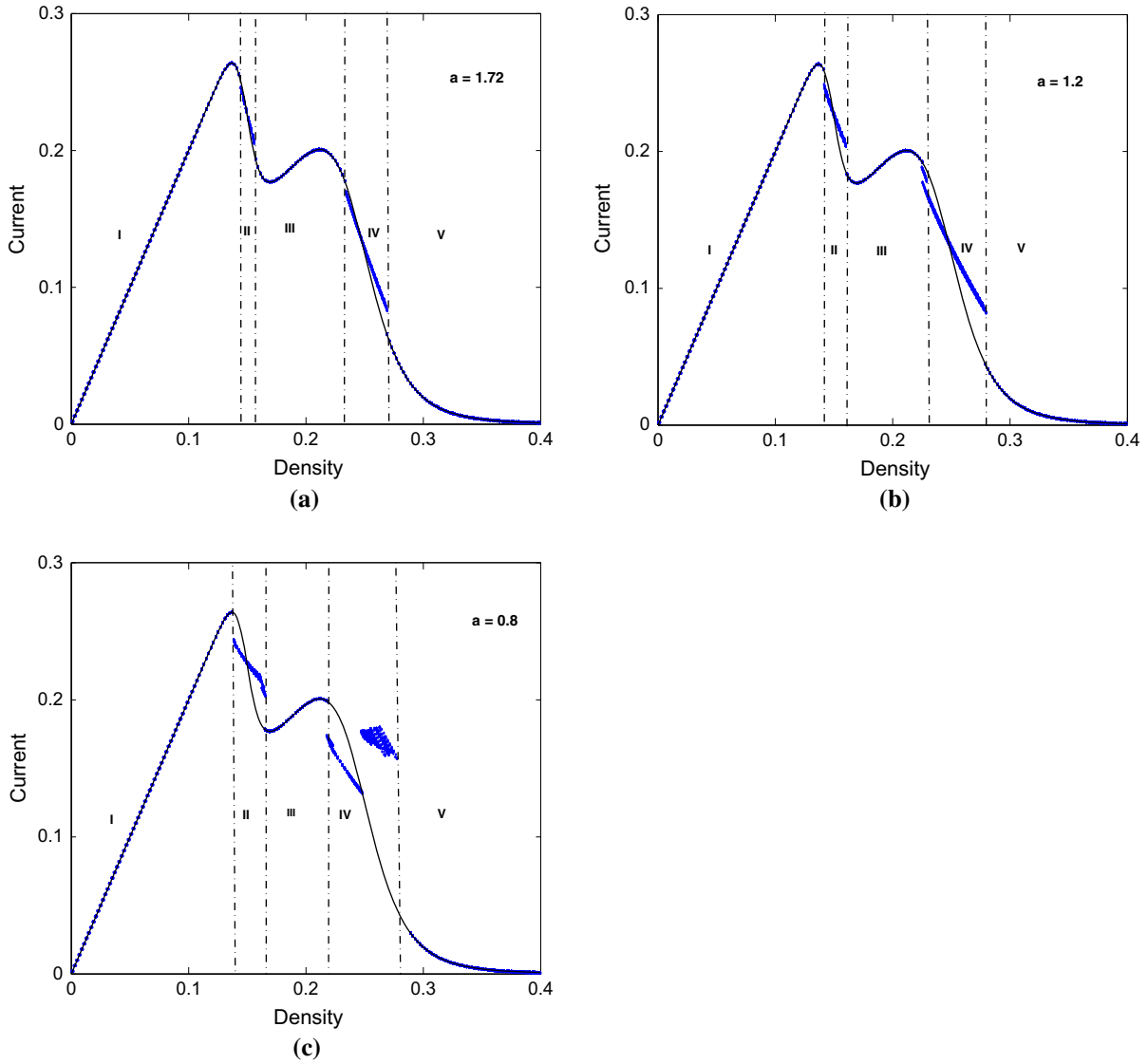

Fig. 7 Plots of flow $q(t)$ versus density $\rho(t)$, when $\lambda = 0$, correspond to the panels in Fig. 3, respectively

Figures 5 and 6 show the plot of instant current $J_j(t)$ against instant density $\rho_j(t)$. Here, the solid line represents the multi-phase optimal flow-density curve. Since, in a homogeneous traffic, all the fundamental variables are identical, the homogeneous traffic flow is represented by a single point on the dotted curve, while both the inhomogeneous traffic states are represented by a loop (limit cycle) in Figs. 5 and 6. It is due to the fact that the current oscillates around the mean value with constant amplitude. The left and right limit cycles in Figs. 5 and 6 correspond to $\rho_j(0) = 0.15$ and $\rho_j(0) = 0.25$, respectively. The upper and lower points of the limit cycles represent the coexisting phases corresponding to the dynamical behavior of vehicles exhibiting the kink–antikink in Figs. 3 and 4. It can also be deduced from the figure that as the amplitude of density waves reduces with an increase in sensitivity and λ, the limit cycles corresponding to both the coexisting phases shrink leading toward the homogeneous flow.

Now, we analyse the fundamental diagram of traffic flow corresponding to the panel of Figs. 3 and 4. Figures 7 and 8 show the plots of traffic current against density by averaging the number of vehicles passing from lattice site j over sufficiently long time,

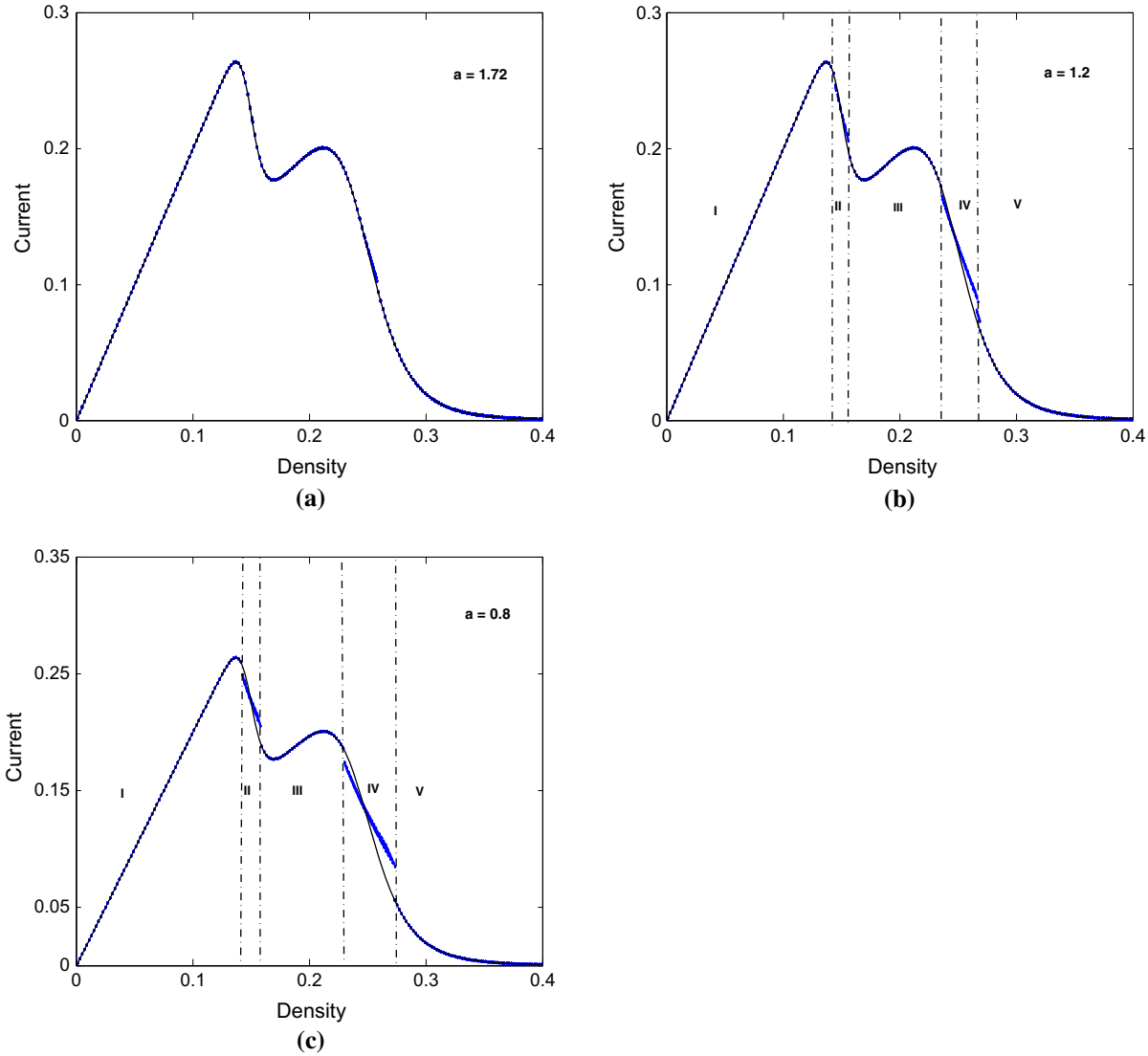

Fig. 8 Plots of flow $q(t)$ versus density $\rho(t)$, when $\lambda = 0.2$, correspond to the panels in Fig. 4, respectively

namely 15,000–20,000 s. The dotted curve represents the theoretical fundamental diagram. For $a > a_c(\lambda)$, the numerical traffic currents completely matches with the theoretical fundamental curve as the density will remain homogeneous spatially. For $a = 1.72$, the simulation results slightly deviates from the theoretical fundamental curve in the coexisting regions. This deviation increases with a decrease in the sensitivity. For $a = 1.2$, the numerical traffic current on one hand matches with the fundamental curve in three different regions representing the free flow, homogeneous intermediate flow and the homogeneous congested flow while on the other hand deviates in two disjoint regions representing the coexisting phases. This deviation is due to the occurrence of traffic jams in these regions. In general, traffic is classified in to five different states as shown in Figs. 7 and 8. It is to be noted that with decreasing sensitivity, the deviation from the theoretical curve increases as more and more stronger traffic jam in the form of high-amplitude kink–antikink density wave is formed. Moreover, the traffic current does not decrease highly with density in the second coexisting region for smaller values of sensitivity. It is to mention that the deviation reduces with an increase in λ. The region of free

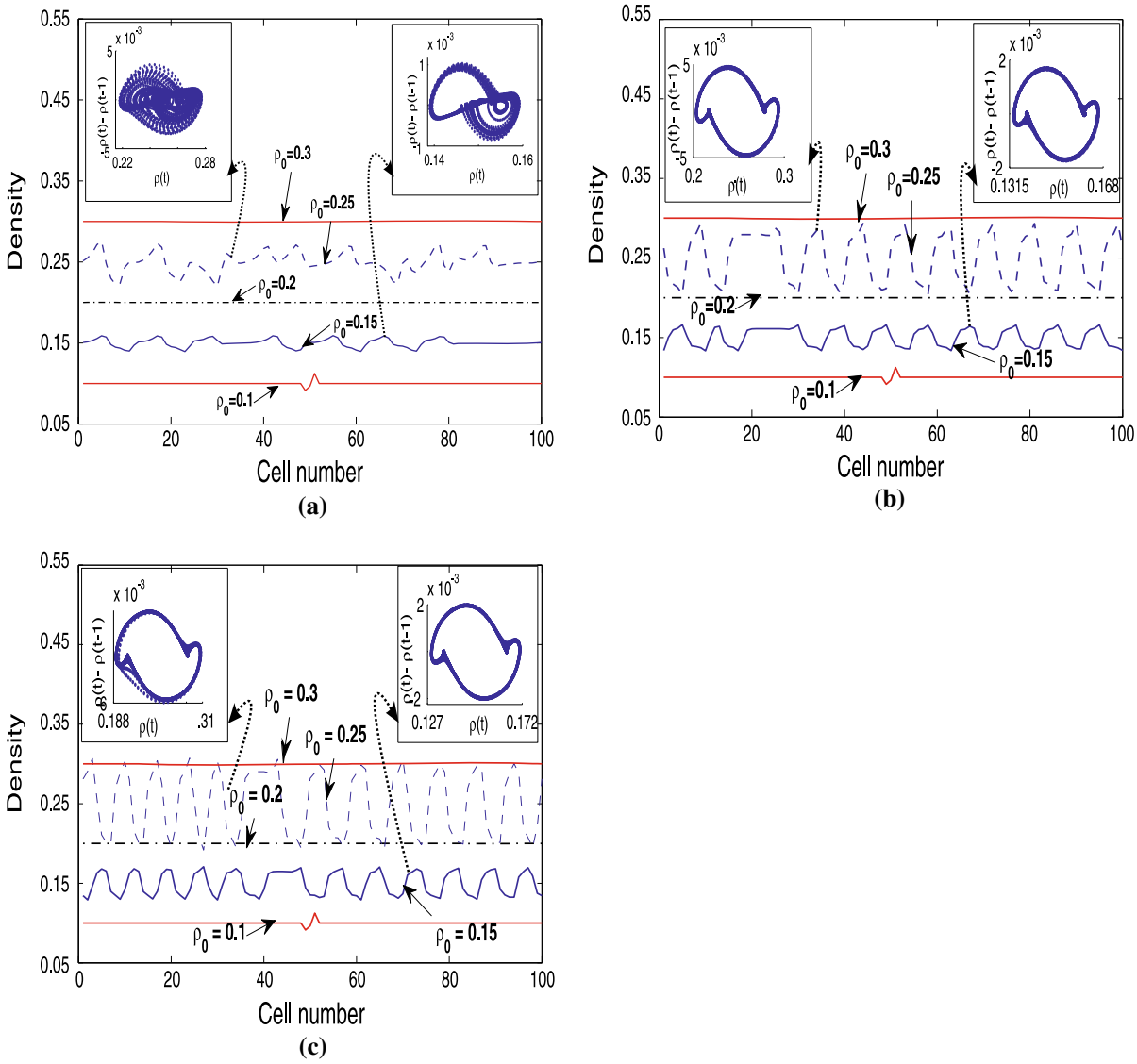

Fig. 9 Density profiles at time $t = 20{,}200$ s when $\gamma = 0.3$ for $\lambda = 0$; **a** $a = 3.5$, **b** $a = 2.5$ and **c** $a = 2.0$, respectively

flow turns wide, and the amplitude of density waves is weakened with the increase in λ, which means that λ enhances the stability of traffic flow even in multi-phase model with passing.

Case 2: $\gamma \geq 0.1667$

We investigate the traffic states by varying the traffic density and sensitivity after sufficiently long time with higher rate of passing ($\gamma = 0.3$). For $a > 5.0$, the traffic flow remains stable against any disturbance in the initial profile. When $a < 5.0$, traffic shows the complex behavior and dynamical phase transitions occur. Figs. 9 and 10 depict the density profile for two different values of $\lambda = 0$ and 0.2, respectively, by varying the initial density as $\rho_0 = 0.1, 0.15, 0.2, 0.25, 0.3$. It is clear from the figures that the pattern of density profiles is different for small values of a as compare to those for larger value of a. Contrary to the case I, based on the sensitivity, two different types of phase transitions occur in four stages. The tri-stable phases, i.e., phase I, II and III, exist for any value of sensitivity and λ. While in the unstable region that is represented by the coexisting phase of phases I, II and II, III, the nature of the den-

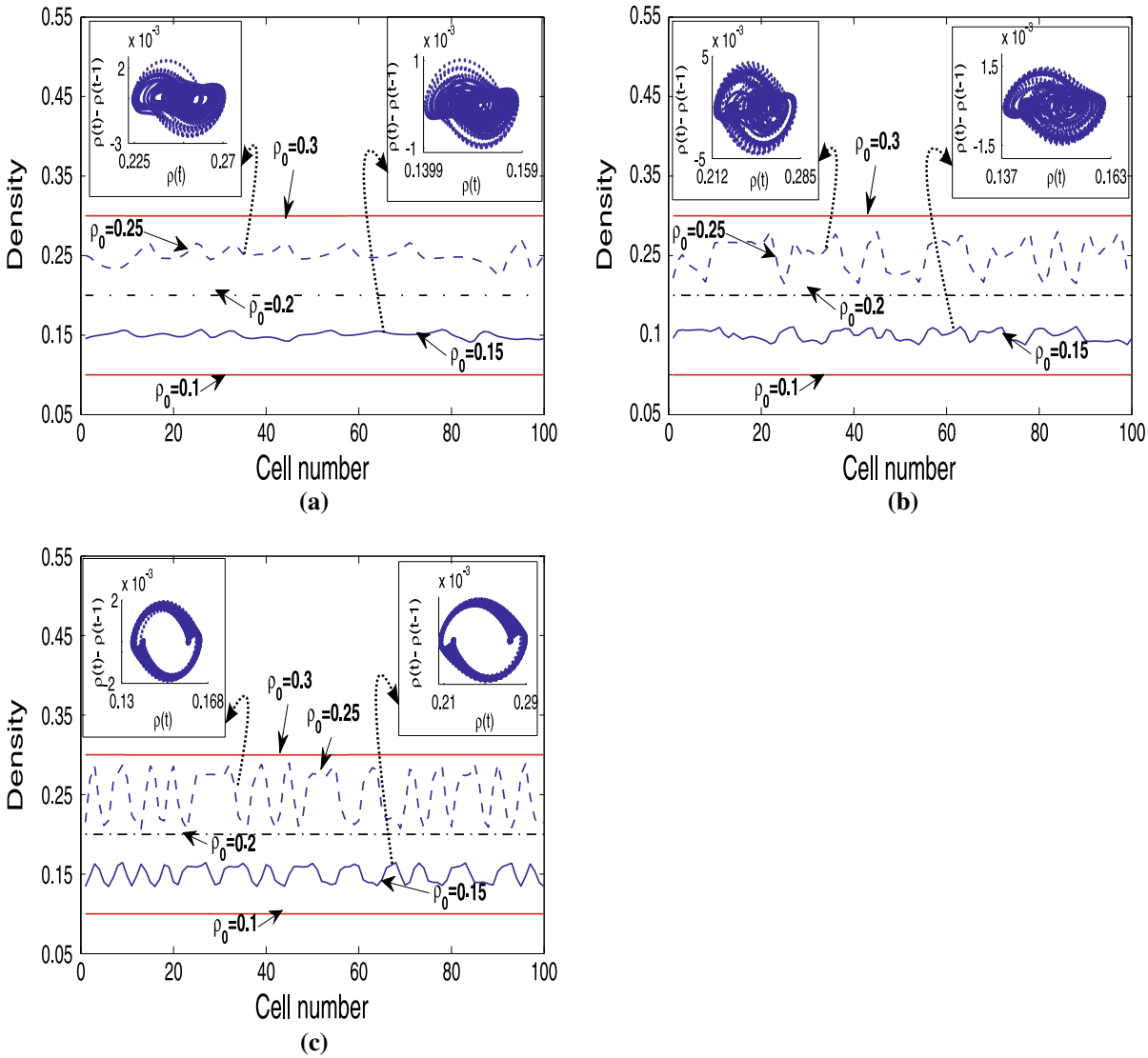

Fig. 10 Density profiles at time $t = 20{,}200$ s when $\gamma = 0.3$ for $\lambda = 0.2$; **a** $a = 3.5$, **b** $a = 2.5$ and **c** $a = 2.0$, respectively

sity profile depends on the sensitivity. For larger values of the sensitivity in both the coexisting phase, the density waves band with one another, break up and propagate in backward direction, resulting in the chaotic flow. When sensitivity becomes smaller than a critical value, the unstable traffic flow is represented by kink–antikink density waves. It is also clear from the Fig. 2 that the critical value of sensitivity decreases with an increase in λ. Here, the traffic displays characteristics of three-phase traffic along with two distinct coexisting phases depending on sensitivity. Parallel to the case I, λ plays a stabilizing role on the density waves as the amplitude of the density wave decreases with λ for any value of sensitivity. It is also clear from the Figs. 9 and 10 that the amplitude of the kink–antikink and chaotic density waves in the second coexisting region is always larger than that of in the first coexisting region for any value of λ and sensitivity.

To further classify traffic states, we draw phase-space plots of density difference $\rho(t) - \rho(t-1)$ against $\rho(t)$ for $t = 15{,}000 - 20{,}000$ s, in the inset of Figs. 9 and 10. The pattern in the inset of Fig. 9c represents the set of dispersed points in the phase-space plot. For larger values of a, the pattern exhibits the limit cycle

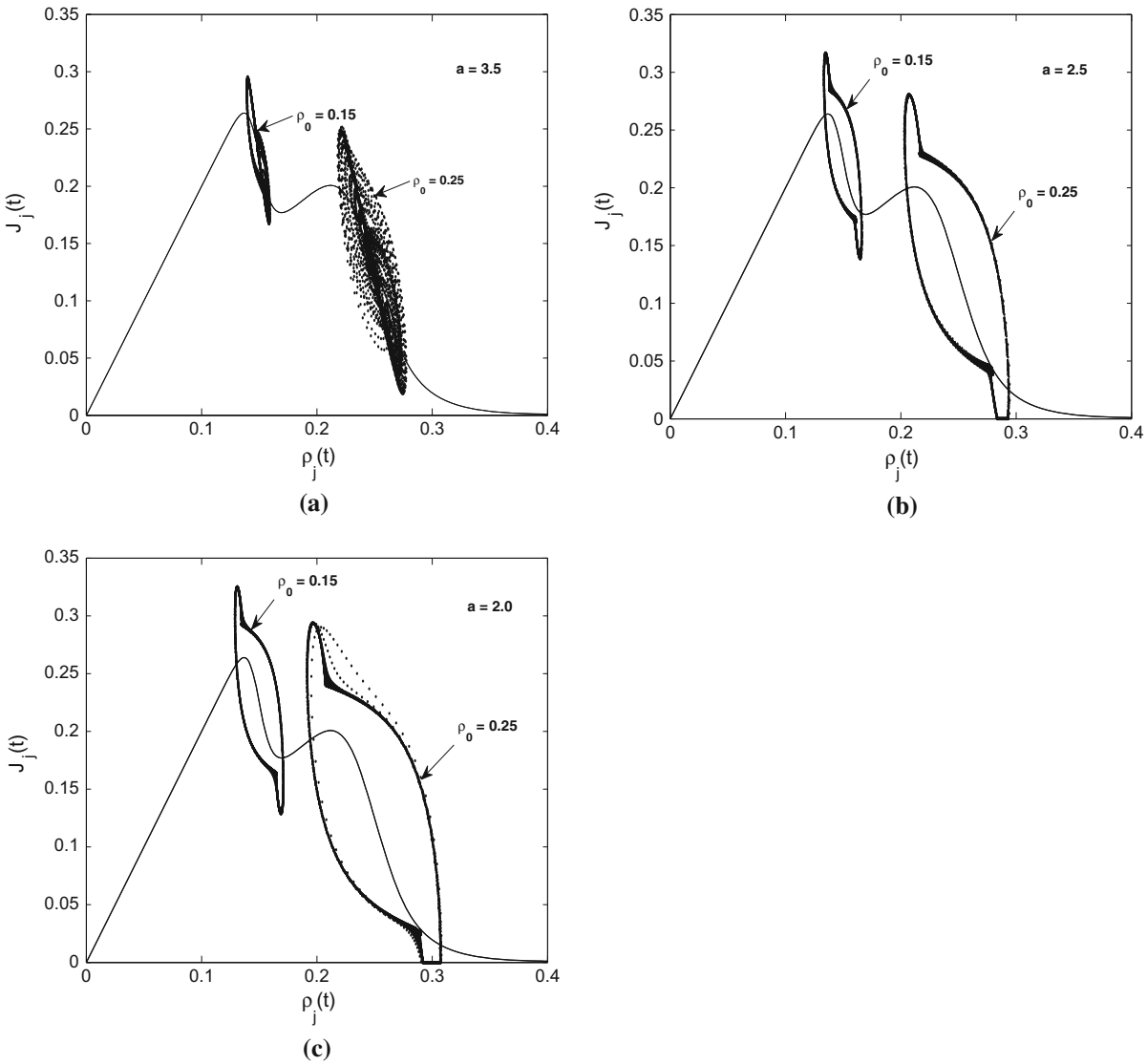

Fig. 11 Plot of $q_j(t)$ against $\rho_j(t)$ when $\gamma = 0.3$ for $\lambda = 0$; **a** $a = 3.5$, **b** $a = 2.5$ and **c** $a = 2.0$, respectively

shown in Figs. 9a and 10a–b. It corresponds to the periodic traffic behavior. As the sensitivity increases, the pattern exhibits dispersed plots around a closed loop, which corresponds to the irregular traffic behavior. This chaotic behavior exhibits the characteristics of chaos. The points on the right and left ends represent, respectively, the states within the traffic jams and within the freely moving phase. It is also clear from the Figs. 9 and 10 that the traffic flow becomes chaotic for relatively smaller values of a when λ is large. Moreover, The amplitude of density waves decreases with an increase in λ in both types of coexisting regions. From these results, we can conclude that kink as well as chaotic region exist in the unstable region on the phase plane which also satisfies theoretical results shown in Fig. 2.

Now, we analyse the effect of λ and sensitivity on instant current $J_j(t)$ with respect to instant density $\rho_j(t)$. Figs. 11 and 12 show the variation of instant current $J_j(t)$ against instant density $\rho_j(t)$ with time corresponding to the panel of Figs. 9 and 10, respectively. When the sensitivity is smaller than the critical value, the density waves are of kink–antikink type and the traffic flow is represented by a limit cycle as

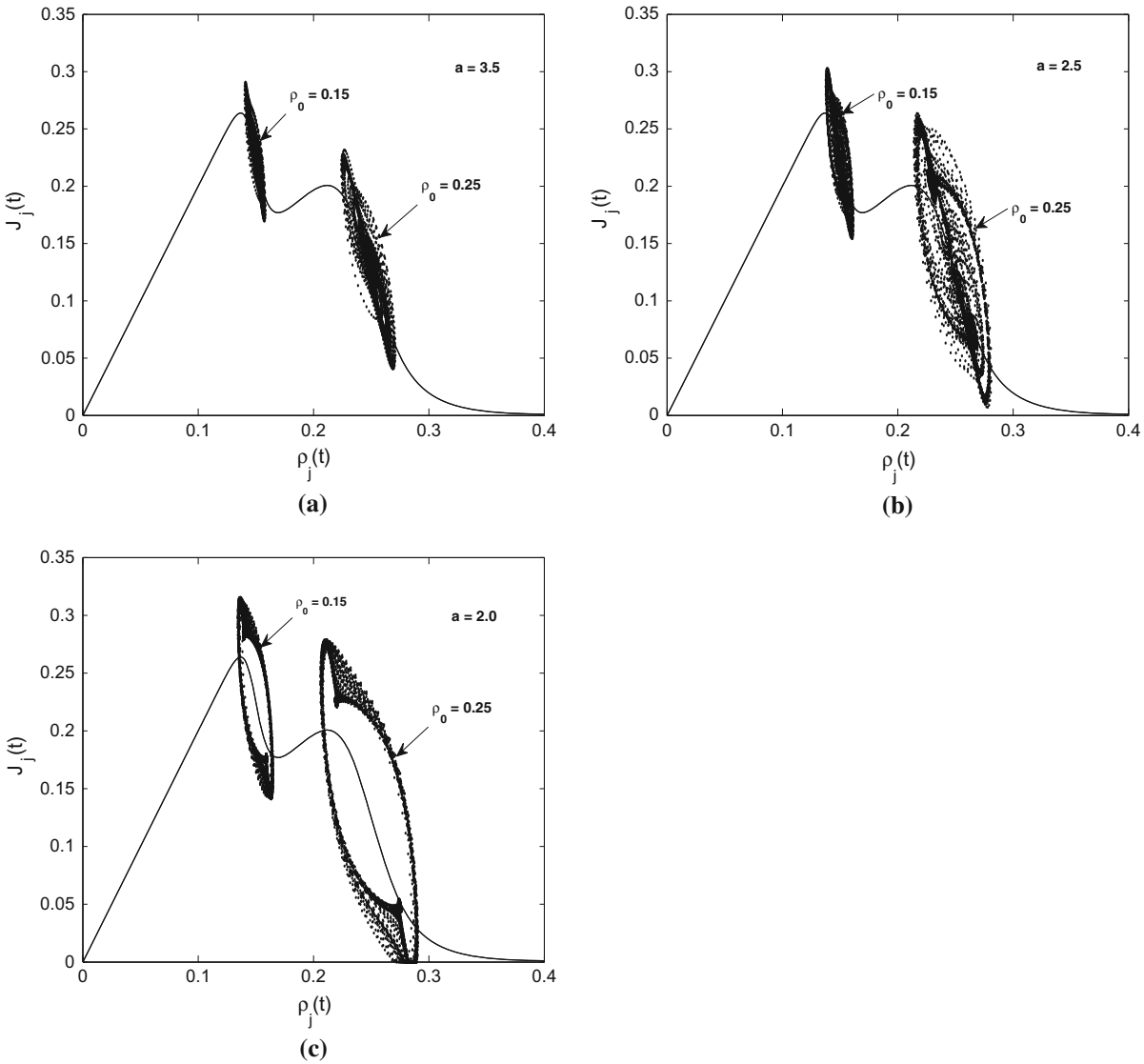

Fig. 12 Plot of $q_j(t)$ against $\rho_j(t)$ when $\gamma = 0.3$ for $\lambda = 0.2$; **a** $a = 3.5$, **b** $a = 2.5$ and **c** $a = 2.0$, respectively

shown in Figs. 11b–c and 12c, where the left and right loops correspond to $\rho_j(0) = 0.15$ and $\rho_j(0) = 0.25$, respectively. When the sensitivity becomes larger than the critical value, the density waves are chaotic in nature and the traffic flow is represented by dispersed plots around a closed loop as shown in Figs. 11a and 12a–b. Points in this region represent the coexisting phases corresponding to the dynamical behavior of vehicles exhibiting the chaotic wave in Figs. 9 and 10. It is to be noted that since the amplitude of density waves in both the coexisting phases reduces with an increase in sensitivity and λ, the limit cycle and chaotic region approach to a single point on the fundamental curve.

Figures 13 and 14 show the plots of traffic current against density by averaging the number of vehicles passing from lattice site-j over sufficiently long time, namely $15{,}000 - 20{,}000$ s. For $a > a_c(\lambda)$, the numerical traffic current completely matches with the theoretical fundamental curve as the density will remain homogeneous spatially. For $a \leq a_c(\lambda)$, the numerical traffic current on one hand matches with the fundamental curve in three different regions representing the free flow, homogeneous intermediate flow and the homo-

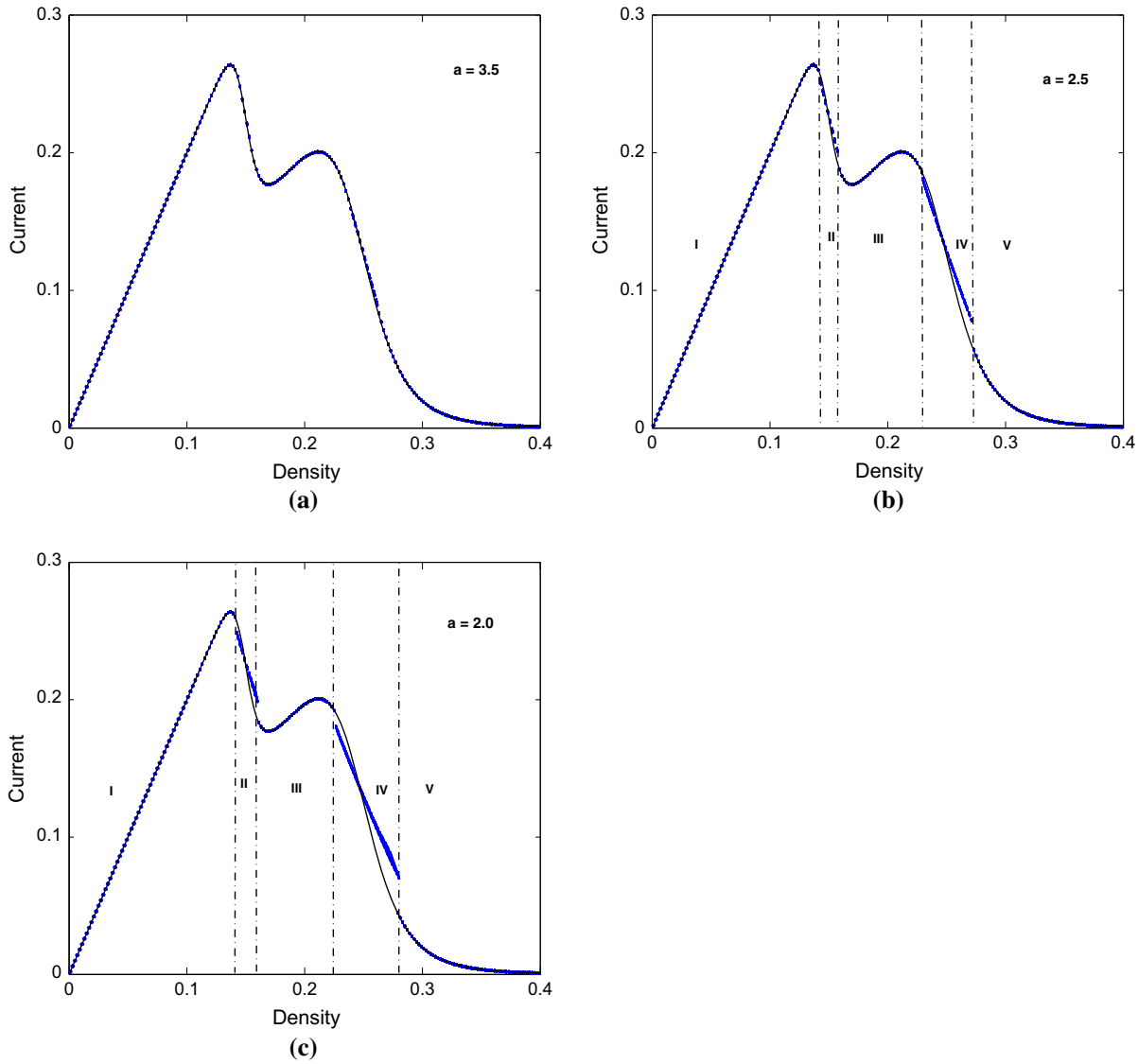

Fig. 13 Plots of flow $q(t)$ versus density $\rho(t)$, when $\lambda = 0$, correspond to the panels in Fig. 9, respectively

geneous congested flow while on the other hand deviates in two disjoint regions representing the coexisting phases. In this case, traffic is also classified into five different states as shown in Figs. 13 and 14. The deviation from the theoretical curve increases with decreasing sensitivity, as more and more stronger traffic jam in the form of high-amplitude kink–antikink or chaotic density wave is formed. The deviation reduces with an increase in λ even in the case of higher rate of passing.

Therefore, it is reasonable to conclude that the multi-phase optimal velocity function plays a significant role in one-dimensional lattice hydrodynamic model with passing. The results also imply that the reaction coefficient can stabilize the traffic flow effectively in a multi-phase lattice hydrodynamic model for all possible rates of passing.

6 Conclusion

We proposed a new one-dimensional density difference lattice hydrodynamic model of traffic flow with passing by incorporating multi-phase optimal veloc-

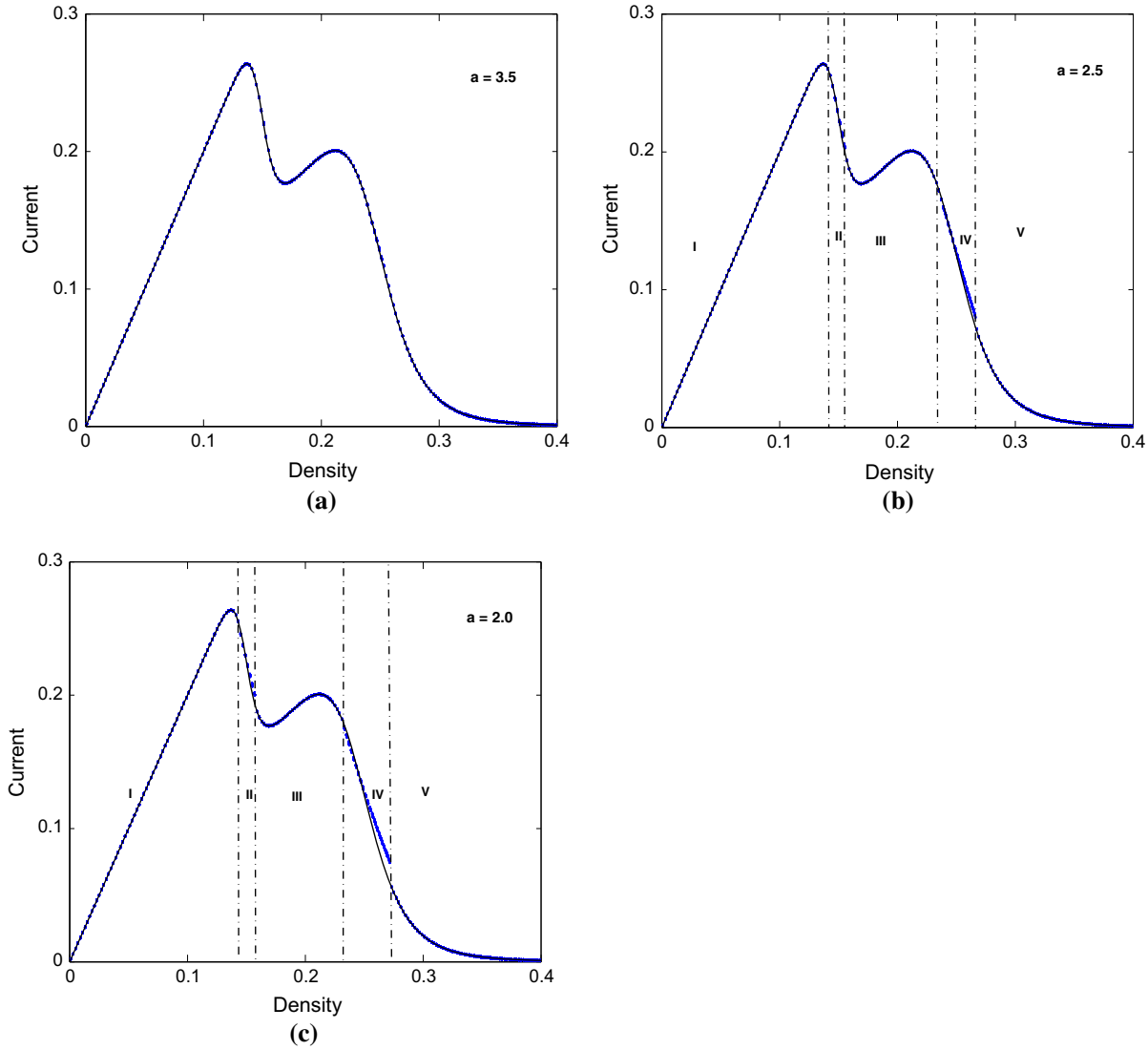

Fig. 14 Plots of flow $q(t)$ versus density $\rho(t)$, when $\lambda = 0.2$, correspond to the panels in Fig. 10, respectively

ity function. The nature of traffic flow has been analyzed through linear and nonlinear analysis. The existence of multi-critical points is shown. Through nonlinear stability analysis, we derived the mKdV equation to describe the traffic jam near the critical point and found the condition for which kink soliton solution of mKdV equation exists. The effect of multi-phase optimal velocity function with two turning points on density waves as well as on fundamental diagram with respect to sensitivity has been discussed for smaller and larger rate of passing. It is concluded that model with two turning points displays three-phase traffic and exhibits multiple phase transitions with increasing density. Based on the passing rate, the complex behavior of traffic flow is explained in terms of multiple phase transitions. We have shown that the reaction coefficient significantly enhances the stability of traffic flow for any value of passing constant even in the case of multi-phase optimal velocity model. The simulation results are compared and found in good accordance with the theoretical findings, which verifies that our consideration is reasonable.

Acknowledgments The third author acknowledges Council of Scientific and Industrial Research, India, for providing financial assistance.

References

1. Chowdhury, D., Santen, L., Schadschneider, A.: A statistical physics of vehicular traffic and some related systems. Phys. Rep. **329**, 199 (2000)
2. Gupta, A.K., Dhiman, I.: Asymmetric coupling in two-lane simple exclusion processes with Langmuir kinetics: Phase diagrams and boundary layers. Phys. Rev. E **89**, 022131 (2014)
3. Gupta, A.K., Dhiman, I.: Coupling of two asymmetric exclusion processes with open boundaries. Phys. A **392**, 6314 (2013)
4. Gupta, A.K., Katiyar, V.K.: Analyses of shock waves and jams in traffic flow. Phys. A **38**, 4069 (2005)
5. Gupta, A.K., Katiyar, V.K.: Phase transition of traffic states with an on-ramp. Phys. A **371**, 674 (2006)
6. Berg, P., Mason, A., Woods, A.: Continuum approach to car-following models. Phys. Rev. E **61**, 1056 (2000)
7. Jiang, R., Wu, Q.S., Zhu, Z.J.: A new continuum model for traffic flow and numerical tests. Transp. Res. Part B Methodol **36**, 405 (2002)
8. Tang, T.Q., Huang, H.J., Gao, Z.Y.: Stability of the car-following model on two lanes. Phys. Rev. E **72**, 066124 (2005)
9. Nagatani, T.: TDGL and MKdV equations for jamming transition in the lattice models of traffic. Phys. A **264**, 581 (1999)
10. Nagatani, T.: Jamming transition in a two-dimensional traffic flow model. Phys. Rev. E **59**, 4857 (1999)
11. Gupta, A.K., Redhu, P.: Jamming transition of a two-dimensional traffic dynamics with consideration of optimal current difference. Phys. Lett. A **377**, 2027 (2013)
12. Peng, G.H.: A new lattice model of traffic flow with the consideration of individual difference of anticipation driving behavior. Commun. Nonlinear Sci. Numer. Simul. **18**, 2801 (2013)
13. Gupta, A.K., Redhu, P.: Analyses of the drivers anticipation effect in a new lattice hydrodynamic traffic flow model with passing. Nonlinear Dyn. **76**, 1001 (2014)
14. Gupta, A.K., Sharma, S., Redhu, P.: Analyses of lattice traffic flow model on a gradient highway. Commun. Theor. Phys. **62**, 393 (2014)
15. Nagatani, T.: Modified KdV equation for jamming transition in the continuum models of traffic. Phys. A **261**, 599 (1998)
16. Tian, J.F., Yuan, Z.Z., Jia, B., Li, M.H., Jiang, G.J.: The stabilization effect of the density difference in the modified lattice hydrodynamic model of traffic flow. Phys. A **391**, 4476 (2012)
17. Ge, H.X., Cheng, R.J.: The backward looking effect in the lattice hydrodynamic model. Phys. A **387**, 6952 (2008)
18. Peng, G.H., Cai, X.H., Cao, B.F., Liu, C.Q.: Non-lane-based lattice hydrodynamic model of traffic flow considering the lateral effects of the lane width. Phys. Lett. A **375**, 2823 (2011)
19. Nagatani, T.: Chaotic jam and phase transition in traffic flow with passing. Phys. Rev. E **60**, 1535 (1999)
20. Peng, G.H., Cai, X.H., Liu, C.Q., Tuo, M.X.: A new lattice model of traffic flow with the anticipation effect of potential lane changing. Phys. Lett. A **376**, 447 (2011)
21. Nagatani, T.: Jamming transitions and the modified Korteweg-de Vries equation in a two-lane traffic flow. Phys. A **265**, 297 (1999)
22. Peng, G.H.: A new lattice model of two-lane traffic flow with the consideration of optimal current difference. Commun. Nonlinear Sci. Numer. Simul. **265**, 297 (2012)
23. Gupta, A.K., Redhu, P.: Analysis of a modified two-lane lattice model by considering the density difference effect. Commun. Nonlinear Sci. Numer. Simul. **19**, 1600 (2013)
24. Peng, G.H.: A new lattice model of the traffic flow with the consideration of the driver anticipation effect in a two-lane system. Nonlinear Dyn. **73**, 1035 (2013)
25. Gupta, A.K., Redhu, P.: Analyses of drivers anticipation effect in sensing relative flux in a new lattice model for two-lane traffic system. Phys. A **392**, 5622 (2013)
26. Kerner, B.S.: The Physics of Traffic. Springer, Heidelberg (2004)
27. Nagatani, T.: Multiple jamming transitions in traffic flow. Phys. A **290**, 501 (2001)
28. Nagai, R., Nagatani, T., Yamada, A.: Phase diagram in multi-phase traffic model. Phys. A **355**, 530 (2005)
29. Li, X., Li, Z., Han, X., Dai, S.: Effect of the optimal velocity function on traffic phase transitions in lattice hydrodynamic models. Commun. Nonlinear Sci. Numer. Simul. **14**, 2171 (2013)